

**SULFURIC ACID PRODUCTION ON EUROPA:
THE RADIOLYSIS OF SULFUR IN WATER ICE**

R. W. Carlson¹, M. S. Anderson¹, R. E. Johnson², M. B. Schulman¹, and A. H. Yavrouian¹

¹Jet Propulsion Laboratory, California Institute of Technology, Pasadena, CA 91109

²University of Virginia, Charlottesville, VA 22903

Submitted to *Icarus*, October 4, 2001

Revised, 27 January 2002

28 manuscript pages

1 table

4 figures

Proposed running head: SULFURIC ACID PRODUCTION ON EUROPA

Corresponding author:

Robert W. Carlson

Jet Propulsion Laboratory 183-601

4800 Oak Grove Drive

Pasadena, CA 91109

Tel: 818-354-2648

Fax: 818-393-3218

E-mail: rcarlson@lively.jpl.nasa.gov

Abstract

Europa's surface is chemically altered by radiolysis from energetic charged particle bombardment. It has been suggested that hydrated sulfuric acid ($\text{H}_2\text{SO}_4 \cdot n\text{H}_2\text{O}$) is a major surface species and is part of a radiolytic sulfur cycle, where a dynamic equilibrium exists between continuous production and destruction of sulfur polymers S_x , sulfur dioxide SO_2 , hydrogen sulfide H_2S , and $\text{H}_2\text{SO}_4 \cdot n\text{H}_2\text{O}$. We measured the rate of sulfate anion production for cyclo-octal sulfur grains in frozen water at temperatures, energies, and dose rates appropriate for Europa using energetic electrons. The measured rate is $G_{\text{Mixture}}(\text{SO}_4^{2-}) = f_{\text{Sulfur}} (r_0/r)^\beta G_1$ molecules $(100 \text{ eV})^{-1}$, where f_{Sulfur} is the sulfur weight fraction, r is the grain radius, $r_0 = 50 \text{ }\mu\text{m}$, $\beta \approx 1.9$, and $G_1 = 0.4 \pm 0.1$. Equilibrium column densities N are derived for Europa's surface and follow the ordering $N(\text{H}_2\text{SO}_4) \gg N(\text{S}) > N(\text{SO}_2) > N(\text{H}_2\text{S})$. The lifetime of a sulfur atom on Europa's surface for radiolysis to H_2SO_4 is $\tau(-\text{S}) = 120(r/r_0)^\beta$ years. Rapid radiolytic processing hides the identity of the original source of the sulfurous material, but Iogenic plasma ion implantation and an acidic or salty ocean are candidate sources. Sulfate salts, if present, would be decomposed in < 3800 years and be rapidly assimilated into the sulfur cycle.

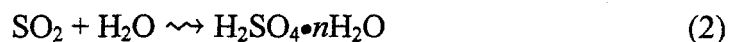
Keywords: Europa; radiation chemistry; surfaces-satellite, magnetospheres

INTRODUCTION

Europa, the innermost icy galilean satellite, orbits within Jupiter's giant magnetosphere and is continuously bombarded by energetic ions and electrons that profoundly influence the chemical composition of the surface. Implantation of Iogenic sulfur ions provides a source of chemically active surface material, and high-energy particles decompose surface molecules and produce new chemical species. Radiolysis is shown to occur on Europa's surface by the presence of hydrogen peroxide (H_2O_2) (Carlson *et al.* 1999a; Carlson 2001; see laboratory studies by Moore and Hudson 2000) and atmospheric and surficial oxygen (O_2) (Hall *et al.* 1995; Hall *et al.* 1998; Spencer and Klesman 2001). Europa's surface also contains an abundant hydrated compound, suggested to be hydrated sulfuric acid ($\text{H}_2\text{SO}_4 \cdot n\text{H}_2\text{O}$) that is radiolytically produced from sulfur-bearing surface material (Carlson *et al.* 1999b). Elemental sulfur is both a radiolytic source and sink of this sulfuric acid, and sulfur allotropes (S_x) can provide the brownish surface pigment that is spatially associated with the hydrate (Carlson *et al.* 1999b). Although it was suggested earlier that the observed SO_2 (Lane *et al.* 1981; Noll *et al.* 1995) was radiolytically decomposed to a sulfur residue (Johnson *et al.* 1988), the cycling among sulfur species and the role of the important end product, sulfuric acid, were missed.

Sulfuric acid, sulfur, and sulfur dioxide are part of a Europa's radiolytic sulfur cycle (Fig. 1) and, along with water ice, constitute a surface in dynamic equilibrium between continuous

production and destruction by radiation-induced chemical reactions (Carlson *et al.* 1999b). The primary products are:



where \rightsquigarrow denotes radiolysis, *i. e.*, reactions initiated by ionizing radiation. In many cases the specific chemical reactions and stoichiometric relations are unknown. The radiolysis of sulfur in water (Reaction 1) efficiently produces sulfuric acid and no other detectable species (Donaldson and Johnston 1968; DellaGuardia and Johnston 1980), but this reaction has been studied only for room temperature liquid mixtures. It is important to determine the efficacy of radiolysis to form sulfuric acid from sulfur-water ice mixtures at low temperatures relevant to Europa. In the following we report measurements of sulfur radiolysis in water ice and show that H_2SO_4 is rapidly produced in Europa's sulfur cycle.

Fig. 1.

RADIOLYSIS MEASUREMENTS AND RESULTS

Two types of experiments were conducted. We first used a fixed radiation dose but varied the concentration, temperature, and phase of the irradiated samples to obtain the reaction efficiency (G -value) and to compare with liquid-state measurements. We then used constant sample conditions but varied the dose to demonstrate that H_2SO_4 is a primary product and that

the measured efficiency is not influenced by back-reactions. In both cases, sulfuric acid generation was measured by the concentration of the sulfate anion SO_4^{2-} measured by ion chromatography.

Experimental conditions and sample preparation

We prepared frozen samples of sulfur in water and subjected them to high-energy particle fluxes that approximate conditions on Europa. High-energy electrons provide 80% of the radiolyzing energy flux at Europa with a mean electron energy of ~ 350 keV (Cooper *et al.* 2001). The total radiolyzing energy flux $\Phi_E = 7.8 \times 10^{13}$ eV cm^{-2} s^{-1} , deposited in the average stopping distance $D = 0.6$ mm (Cooper *et al.* 2001), gives a surface dose rate of about 20 rad s^{-1} although this rate can be spatially variable (Paranicas *et al.* 2001). Our experiments used recoil electrons produced within the sample by Compton scattering of ^{60}Co γ -rays for which the average recoil energy is ~ 500 keV. The intensities of the two sources that we used were ~ 3.3 rad s^{-1} and ~ 20 rad s^{-1} . Thus, the experimental energy and dose rates both approximate European conditions.

A 500-keV electron impacting water ice has a range $R \approx 3$ mm and produces numerous primary ionization events with an average spacing of ~ 0.5 μm established by the ionization cross section and concentration of H_2O molecules. The secondary electrons produced at each primary site cause further excitation and ionization events, but with shorter range, so small, discrete regions of high energy density are produced. The regions can overlap near the end of the

primary's track and in branch tracks that are produced by energetic secondary electrons.

Dissociative recombination of the e^- - ion pairs and the dissociation of excited molecules produce H and OH radicals within the excitation regions, which are $\sim 20 \text{ \AA}$ in diameter and contain an average of about five dissociated H_2O molecules (Hochanadel 1960). Some radicals recombine to form H_2O , H_2 , and H_2O_2 , but many of the OH radicals can migrate and react with other species or become trapped and available for subsequent reactions. Oxidation of elemental sulfur to sulfuric acid occurs by successive reactions with OH radicals (DellaGuardia and Johnston 1980). Hydrogen peroxide is quite non-reactive with elemental sulfur (Schumb *et al.* 1955) (see below). Other oxidants, produced at lesser rates in ice radiolysis, are O, O_2 , and HO_2 and are discussed below.

Experimental samples were irradiated at $T = 77\text{K}$, a temperature comparable to Europa's nighttime temperature of 86 K (Spencer *et al.* 1999). At these low temperatures, many OH radicals are trapped, with the amount of trapping dependent on the number of defects and hence on the history of the ice (Ershov and Pikaev 1969). Voids at interfaces and grain boundaries provide favorable sites for trapping and chemical reactions (Johnson and Jesser 1997). On warming to $\sim 100 \text{ K}$, OH radicals become quite mobile (see review by Johnson and Quickenden 1997 and references therein) and behave chemically like OH in liquid H_2O (Taub and Eiben 1968). These OH radicals diffuse and react with themselves and other molecules to form more stable products. Experiments show that these reactions are completed and the OH radicals

consumed for $T \lesssim 130$ K (Johnson and Quickenden 1997). This temperature regime, 100 K to 130 K, is within Europa's diurnal temperature range of 86 to 132 K (Spencer *et al.* 1999). We experimentally simulated European temperature conditions by slowly warming the 77 K-irradiated samples through this temperature range ($dT/dt < 1$ K s^{-1}).

Elemental sulfur on Europa's surface may occur in the S_8 cyclo-octal form or as linear chains, S_x , and both may be present as isolated molecules or as aggregates, the case considered here. The laboratory samples were prepared using 99.998+% pure rhombic S_8 flakes ground to finer particles. Ultra pure water (resistivity > 17 M Ω - cm), prepared using a Barnstead NanoPure® ion-exchange system, was used in these experiments. The weight fraction of sulfate impurities, relative to S_8 , was reduced to $\sim 0.4 \times 10^{-6}$ by repeated rinsing. Some nitrate was also present at about the same level in both the sulfur and water. Heterogeneous mixtures were prepared using water that had been degassed by boiling for 30 min and stored in a glass bottle with no headspace. Sulfur and water were weighed into 6-ml high-density polyethylene vials. The vials were capped and sonicated for 15 minutes to disperse the sulfur and further de-aerate the mixture, and then immersed in the cryogen.

G-value measurements

Radiolytic efficiencies are often expressed as G -values, the number of molecules produced (or destroyed) per 100-eV of absorbed energy. Typical values are $G = 0.1$ to 10 and are generally higher in the liquid state than in solids. They depend on the energy and type of ionizing

particle, but sparsely ionizing, very fast particles are often treated as similar (Johnson and Quickenden 1997).

We measured the G -value for sulfate production using a donut-shaped ^{60}Co source. With this geometry, the dose rate ($\sim 3.3 \text{ rad s}^{-1}$) is uniform in the central sample region. External access is precluded during irradiation, so cooling must be accomplished using cryogenics such as liquid nitrogen and CO_2 ice. For each measurement set, we prepared samples two sets of solutions at four concentration levels ($f_{\text{Sulfur}} = 0\%, 5\%, 10\%, \text{ and } 15\%$, by mass). One set was irradiated while the other set received similar thermal treatment in an identical dewar but was not irradiated. The sulfur particle size distribution was optically determined using a representative sample of > 5000 particles and counting the number of particles classified by size ranges. A log-normal distribution was found with maximum at radius $r_0 = 50 \mu\text{m}$ and a standard deviation in $\ln(r)$ of 0.4.

After the exposure period, the samples were allowed to warm slowly and melt, followed immediately by chromatographic analysis. We used a Dionex ion chromatograph consisting of a GP40 gradient pump and a CD20 conductivity detector with an anion self-regenerating suppressor operated at 50mV. Separation was accomplished on a Dionex Ion Pac® AS4A-SC column preceded by an Ion Pac® AG4A-SC guard column. The instrument was calibrated before each group of measurements and checked after completion to ensure that there had been

no significant change in detector response. In addition to the unexposed control set, samples of the ultra pure water were also analyzed to validate sample preparation and handling.

Variations in the amounts of generated sulfate of about $\pm 30\%$ were observed for different samples at the same concentration. These differences are thought to arise from different degrees of particle dispersion among otherwise identical samples. Errors in the chromatographic determination of the sulfate concentration are about 0.01 to 0.02 ppm.

Fig. 2.

Irradiations were performed for ~ 8 h (dose ~ 100 krad $\sim 6 \times 10^{18}$ eV g^{-1}) at 77 K and 195 K using liquid nitrogen and dry ice cryogenics, respectively. The chromatograms (e. g. Fig. 2) show that the sulfate weight fraction f_{Sulfate} produced by radiolysis is approximately proportional to f_{Sulfur} , and that production is less for the 195 K irradiation (Fig. 3). Assuming a linear relationship, $f_{\text{Sulfate}} \approx \alpha f_{\text{Sulfur}}$, applicable for $f_{\text{Sulfur}} \ll 1$, least-squares analysis yields $\alpha = 3.9 \pm 0.4$ ppm for the 77 K irradiation, and $\alpha = 0.9 \pm 0.6$ ppm for the 195 K irradiation. The results are consistent with a linear dependence with f_{Sulfur} (for $f_{\text{Sulfur}} \ll 1$) and we include a power law to describe particle size dependence, expressing the radiolytic efficiency as $G_{\text{Mixture}}(\text{SO}_4^{2-}) = f_{\text{Sulfur}} (r_0/r)^\beta G_1$. The parameter $r_0 = 50 \mu\text{m}$ is the mean particle radius in these experiments and the value of β is estimated below. G_1 is found using the measured value of α and the corresponding dose. For the 77 K and 195 K irradiations we find $G_1 = 0.4 \pm 0.1$ molecules $(100 \text{ eV})^{-1}$ and $G_1 = 0.1 \pm 0.07$ molecules $(100 \text{ eV})^{-1}$, respectively. Error estimates include the variances in the fits,

uncertainty in the source strength, and the sample-to-sample variance. The value for the 77 K irradiation is appropriate for Europa's diurnal temperature variation. The lower efficiency for SO_4^{2-} production at 195 K implies that competing reactions with OH are important at this temperature. These reactions may involve thermally enhanced diffusion of previously generated products (Ghormley and Stewart 1956).

Fig. 3.

We also measured SO_4^{2-} production from a liquid aqueous mixture, finding $G_1 = 8$ for 50- μm radius S_8 particles. Previous radiolysis measurements in liquid H_2O (Donaldson and Johnston 1968) yielded $G_{\text{Mixture}} = f_{\text{Sulfur}} (r_0/r)^\beta G_1 = 0.05$ using low sulfur concentration ($f_{\text{Sulfur}} = 0.6$ ppm) and $r = 0.4$ μm radius particles. The different particle sizes used in the two experiments enables us to estimate the parameter β . Combining our value for G_1 with Donaldson and Johnston's value for $G_{\text{Mixture}}/f_{\text{Sulfur}}$ gives $\beta \approx 1.9$. Using $f_{\text{Sulfur}} \propto nr^3$, where n is the particle number density, we find that $G_{\text{Mixture}} \propto nr^{1.1}$. Donaldson and Johnston, in measuring the rates of decrease of sulfur particle radii, found that the corresponding sulfuric acid production rate was midway between two cases: (1) uniform diffusion of radicals to the grain's surface and (2) a constant source volume for the reacting radicals. For the diffusion case $G_{\text{Mixture}} \propto nr^2$, while the constant source volume case is described by $G_{\text{Mixture}} \propto n$. Our independently-derived variation, $G_{\text{Mixture}} \propto nr^{1.1}$, lies between these two cases and is consistent with Donaldson and Johnson's finding. We assume that the particle size dependence will be the same in the solid state.

Oxidants and reaction pathways

Hydrogen peroxide is an oxidant that is generated in the radiolysis of H₂O, so we investigated the direct oxidation of S₈ by H₂O₂. A non-irradiated mixture of S₈ in a 6%-wt aqueous solution of H₂O₂ produced 14×10^{-6} g (SO₄²⁻)/g (S₈) in 20 hours. The average H₂O₂ concentration for the radiolyzed samples is expected to be ~ 0.16 ppm-wt, estimated using $G(\text{H}_2\text{O}_2) = 0.08$ (Johnson and Quickenden 1997). Normalizing the sulfate production to the H₂O₂ levels and exposure times of the irradiated samples, we estimate that H₂O₂ oxidation would give $< 2 \times 10^{-11}$ g (SO₄²⁻)/g (S₈). This is less than 10⁻⁵ of the value for irradiated samples, so we conclude that H₂O₂ probably plays, at most, only a minor role in sulfur oxidation. Indeed, H₂O₂ *inhibits* H₂SO₄ production in irradiated liquid mixtures (Donaldson and Johnston 1968). We also found that the presence of O₂ *inhibits* H₂SO₄ production in ice, similar to Donaldson and Johnston's (1968) results for liquid water. We discuss oxidation by HO₂ in the following subsection.

Our results are consistent with successive oxidation by OH and probably similar to OH oxidation of S₈ in irradiated liquid mixtures (DellaGuardia and Johnston 1980). Both phases may involve the sulfoxylate ion, SO₂²⁻, (Vairavamurthy and Zhou 1995) and sulfinic acid, SO₂H₂, (DellaGuardia and Johnston 1980) as intermediates. SO₂H₂ is produced in low temperature (12 K) photolysis (Fender *et al.* 1991) and sulfinic acids are oxidized to sulfate (Makarov *et al.* 1998). The final step, hydration of sulfuric acid, is highly exothermic and may occur

simultaneously with three-body oxidation reactions. For low sulfate-to-water ratios, the octahydrate and hemihexahydrate would be formed.

Dose dependence

The *primary products* of radiolysis are the stable end-products that result from reactions of the initial radicals with the molecules present before irradiation. With increased dose, the concentration of primary products will increase and can participate in subsequent radiolytic reactions (“back reactions”), producing *secondary products* through the decomposition of the primary products. One can experimentally distinguish between primary and secondary products through their dose dependence. The concentration of primary products will initially be proportional to dose but will reach a dose-independent plateau at high doses, where net production and destruction rates are equal. Secondary products will first exhibit a quadratic dependence, becoming linear with a non-zero dose rate offset at higher doses (O'Donnell and Sangster 1970).

The relative amount of sulfate generated in the above exposures is small, being in the parts-per-million range for the ~ 100 krad exposures. Therefore the destruction of H₂SO₄ molecules is expected to be small compared to the number being produced, so the measured *G*-value should represent the primary product yield. We verified that initial production rates were measured by exposing fixed-concentration samples to various total doses. Samples with $f_{\text{Sulfur}} = 15\%$ were prepared as described above and maintained at 77 K while being exposed at 20-rad s⁻¹

from a “point” source of ^{60}Co γ -rays. Similarly prepared control samples experienced the same thermal environment but were unexposed. Exposures times ranged from ~ 4 h to 72 h (dose ~ 0.3 to 5 Mrad) and the amount of sulfate that was generated is consistent with a linear dose dependence with no offset (Fig. 4), as expected for primary product generation and negligible back reactions.

Fig. 4.

These data also show that HO_2 is not a major oxidant in sulfur + ice radiolysis. The hydroperoxyl radical is a secondary product generated from the primary product H_2O_2 ($\text{OH} + \text{H}_2\text{O}_2 \rightarrow \text{HO}_2 + \text{H}_2\text{O}$) so HO_2 , and any of its oxidation products, should exhibit a quadratic dose dependence. Such dependence is not observed (Fig. 4).

IMPLICATIONS FOR EUROPA

Reaction rates, lifetimes, and relative concentrations

It is important to determine the rate, and characteristic time, for conversion of sulfur in ice into the hydrated H_2SO_4 seen on Europa. Consider the general case of species X radiolyzed to products Y . The column density of molecules X above the stopping depth D is $N(X) = (f_X \langle \rho \rangle / m_X) D$, where $\langle \rho \rangle$ is the mean density, and m_X and f_X are the mass and mass fractions of molecule X . The stopping distance varies inversely with density, so we use $D = D_{\text{Ice}} (\rho_{\text{Ice}} / \langle \rho \rangle)$ and Cooper et al.’s value of $D_{\text{Ice}} = 0.62$ mm for $\rho_{\text{Ice}} = 1$ g cm^{-3} . Ignoring back reactions, species Y is produced at the rate

$$dN(Y)/dt \equiv N(X)v(X \rightarrow Y) = f_X(r_0/r)^\beta G_1(Y)\Phi_E/(100\text{eV}),$$

giving the rate per molecule v as

$$v(X \rightarrow Y) = m_X (r_0/r)^\beta G_1(Y)\Phi_E/[(100\text{eV})D_{\text{Ice}}\rho_{\text{Ice}}].$$

We have included the size dependence term $(r_0/r)^\beta$ for heterogeneous mixtures; it is to be replaced by unity for homogeneous samples. Summing $(r_0/r)^\beta G_1$ for all independent products produced in the decomposition of X gives the G -value for destruction, $G_1(-X)$. The rate of destruction, $v(-X)$, and corresponding lifetime, $\tau(-X)$, for molecule X are:

$$v(-X) = 1/\tau(-X) = m_X G_1(-X)\Phi_E/[(100\text{eV})D_{\text{Ice}}\rho_{\text{Ice}}]$$

The end product of sulfur:H₂O radiolysis is H₂SO₄, so $G_1(-S) = (r_0/r)^\beta G_1(\text{H}_2\text{SO}_4)$, giving the S atom lifetime $\tau(-S) = 120$ y for 50- μm radius particles. Sulfur is continuously being replenished by radiolytic destruction (back reactions) of H₂SO₄, SO₂, and H₂S (Fig. 1).

Table I

We use current and previous measurements (Table I) to estimate production and destruction rates at Europa and the resulting concentrations of S, SO₂, and H₂S, relative to H₂SO₄. Sulfate acids and salts are decomposed by cation reduction or ejection and by decomposition of the sulfate anion. The sulfuric acid cations (H⁺, H₃O⁺, H₅O₂⁺) can be reformed relatively quickly since H₂O is abundant. Sulfate anion radiolysis products are elemental sulfur, sulfides, and sulfites (Sasaki *et al.* 1978), yielding S, H₂S, and H₂SO₃ (sulfurous acid). Sulfurous acid dissociates as $2\text{H}^+ + \text{SO}_3^{2-} \rightleftharpoons \text{H}^+ + \text{HSO}_3^- \rightleftharpoons \text{SO}_2 + \text{H}_2\text{O}$ with the latter case being favored

at the low pH level of Europa's surface (Martin and Damschen 1981). Because the surface O₂ density is not known, we do not include oxidation of S by O₂, but this pathway can produce SO₂ and H₂SO₄ as in Venus's atmosphere (Yung and DeMore 1982). Photodissociation of SO₂ and H₂S by solar ultraviolet radiation will increase their destruction rates, but photoabsorption by H₂O and sulfur provides some spectral shielding, particularly for SO₂. Ignoring photodissociation, the equilibrium molar ratios are:

$$N(S)/N(H_2SO_4) = [v(H_2SO_4 \rightarrow SO_2)/v(-SO_2)] [v(SO_2 \rightarrow S)/v(-S)] +$$

$$[v(H_2SO_4 \rightarrow H_2S)/v(-H_2S)] [v(H_2S \rightarrow S)/v(-S)] + v(H_2SO_4 \rightarrow S)/v(-S).$$

$$N(SO_2)/N(H_2SO_4) = v(H_2SO_4 \rightarrow SO_2)/v(-SO_2)$$

$$N(H_2S)/N(H_2SO_4) = v(H_2SO_4 \rightarrow H_2S)/v(-H_2S)$$

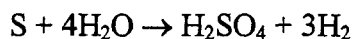
Using the values in Table I we find that S, SO₂, and H₂S concentrations, relative to H₂SO₄, are in the ratios $10^{-2}(r/50 \mu\text{m})^{1.9}$, 10^{-3} , and 2×10^{-4} , respectively. Hydrated sulfuric acid is the dominant species on the trailing side of Europa and the number of sulfate ions relative to water molecules is ~ 0.1 (Carlson *et al.* 1999b). The corresponding number densities of S, SO₂, and H₂S in a 0.6 mm thick layer are $2 \times 10^{18}(r/50 \mu\text{m})^{1.9}$, 2×10^{17} , and $4 \times 10^{16} \text{ cm}^{-2}$. Observations of SO₂ on Europa's trailing side (Noll *et al.* 1995) are consistent with this estimate (Carlson *et al.* 1999b). Sulfur atoms can combine to form long-chained polymers S_x that are highly absorbing in the visible ("red sulfur") (Meyer *et al.* 1971) and can color Europa's surface, even at trace levels

of 10^{-4} (Clark and Lucey 1984). The H_2S ν_3 band at $3.9 \mu\text{m}$ is not apparent in Near Infrared Mapping Spectrometer (NIMS) spectra of Europa, consistent with these predictions

The above concentration ratios are lower limits. If the surface becomes saturated in sulfuric acid hydrate, with no free H_2O molecules available to supply oxygen for sulfate production, then acid production will cease and the sulfur concentration can increase. A saturated surface could be significantly darker.

Long-term sulfur cycle imbalance

Although the sulfur cycle is established in a few thousand years and is reversible in a closed system, Europa's surface is an open system. Species more volatile than H_2O , such as H_2 , O_2 , and SO_2 , readily enter the atmosphere where they can be redistributed and buried or lost to space. Loss of H_2 occurs by Jeans' escape and loss of O_2 occurs by ionization (Johnson *et al.* 2000), whereas SO_2 , ejected by sputtering or sublimation, is redistributed like H_2O . Ignoring the molecular oxygen pathways, the net reactions of the sulfur cycle are:



Although some of the evolved hydrogen and oxygen can recombine to form H_2O , there can be a longer-term evolution because H_2 and O_2 will leave the system, increasing the concentration of sulfurous material and therefore becoming darker.

Darkening by thermal alteration and the brightening of lineae

Thermal effects can also darken a surface. Heating of the surface will preferentially sublime H_2O since its vapor pressure is much higher than the vapor pressures of S_x and H_2SO_4 , and even modest heating can saturate and then darken a surface. It has been suggested that warm ice diapirs, upwelling in linear cracks, can heat and sublime the adjacent crust to form diffuse margins of dark refractory material – “triple band” lineae (Head *et al.* 1999). NIMS spectral maps of triple bands show that the center bands are icy but the dark margins contain hydrated sulfuric acid, consistent with sulfurous refractory material (Carlson *et al.* 2001).

Once formed, the triple bands appear to brighten with time (Geissler *et al.* 1998).

Regolith processes such as down-slope motion of talus, impact gardening, or the self-burial of darker, warmer material in ice (“solar gardening”, Grundy and Stansberry 2000) may produce such changes. A surface can be brightened by a frost covering, but frost formation on a darker, hence warmer, surface may be unlikely. However, adsorption of H_2O , coupled with irradiation, can oxidize the dark sulfur polymers to colorless SO_2 and H_2SO_4 hydrate. In addition, sputtering of SO_2 can reduce the net sulfur content and therefore the amount of radiolytically-equilibrated S_x . The surface will slowly brighten in a time that is long compared to the cycling time of the radiolytic sulfur cycle (Fig. 1).

Initial source of sulfurous material

The rapid processing of the radiolytic sulfur cycle described above hides the original source(s) of sulfur. Ion implantation is a known source (Johnson *et al.* 1988), and the implantation rate (computed from Bagenal's (1994) model) is a factor of 10^3 greater than that from micrometeoroid infall (using Cooper *et al.*'s (2001) mass influx rate and atomic abundance values from Anders and Grevasse (1989). An acidic ocean within Europa may provide sulfuric acid (Kargel, J.S. *et al.* 2001; Marion 2001) while a briny ocean could provide sulfate salts (McCord *et al.* 1999; Kargel, J. S. *et al.* 2000). Radiolytic destruction rates for sulfate salts are not well studied but decomposition processes include both cation and anion destruction. Therefore, the lifetime of a sulfate salt will be less than the 3800-year lifetime of the sulfate anion alone (Table I). Both alkali and alkaline earth cations are reduced by radiolysis (Moorthy and Weiss 1964; Sasaki *et al.* 1978) and excited, neutral, Na and Mg atoms are ejected with similar efficiencies from blödite, $\text{Na}_2\text{Mg}(\text{SO}_4)_2 \cdot 4\text{H}_2\text{O}$ (Nash and Fanale 1977), for example. Neutral Mg is ejected from $\text{MgSO}_4 \cdot x\text{H}_2\text{O}$ (Nash and Fanale 1977). A radiolytic equilibrium between Na_2O , NaOH , MgO , $\text{Mg}(\text{OH})_2$, (Na, Mg) sulfates, and sulfuric acid would result (Johnson 2000). There are insufficient data to predict these ratios, but limits of 3% and 5% have been derived for $\text{Mg}(\text{OH})_2$ and NaOH , respectively (Shirley *et al.* 1999). Sulfate salts, if present, can be rapidly assimilated into Europa's sulfur cycle.

SUMMARY AND CONCLUSIONS

We measured the production of sulfuric acid from radiolysis of sulfur grains in ice at temperatures and dose rates relevant to Europa. Since energetic electrons are the dominant ionizing radiation striking the trailing hemisphere of Europa, we used electrons of comparable energy produced by Compton scattering of ^{60}Co γ -rays. Efficient production of H_2SO_4 was found with the rate depending on the sulfur particle grain sizes. These results show that sulfur on Europa's surface will be radiolyzed to sulfuric acid in time scales of years to hundreds of years, depending upon the grain size.

Continuous radiolytic production and destruction on Europa yields H_2SO_4 as the dominant sulfur compound, with S_x , SO_2 , and H_2S being minor species. The cycle time is about 4000 years, set by the relatively stability of sulfates under irradiation. Radiolytic lifetimes at Europa are short compared to geologic time scales and mask the original sulfur source(s); candidates include ion implantation and an acidic or briny ocean. There can be a net, long-term imbalance in the sulfur cycle, due to loss of H_2O as radiolytically produced H_2 and O_2 . This will enhance the concentration of sulfur compounds, as will thermal processes such as diapiric heating. However, adsorption of H_2O and subsequent radiolytic S_x oxidation, along with sputtering of SO_2 , can counteract this trend and may be responsible for surface brightening phenomena.

ACKNOWLEDGEMENT

We thank W. Neiderheiser for performing the particle-size-distribution measurements.

This work was supported by the Planetary Geology and Geophysics Program of the National Aeronautics and Space Administration. Portions of this work were performed at the Jet Propulsion Laboratory, California Institute of Technology, under contract with NASA.

REFERENCES

- Anders, E., and N. Grevasse 1989. Abundances of the elements: Meteoritic and solar. *Geochim. Cosmochim. Acta* **53**, 197-214.
- Bagenal, F. 1994. Empirical-model of the Io plasma torus - Voyager measurements. *J. Geophys. Res.* **99**, 11043-11062.
- Carlson, R. W. 2001. Spatial distribution of carbon dioxide, hydrogen peroxide, and sulfuric acid on Europa (abstract). *Bull. Amer. Astron. Soc.* **33**, 1125.
- Carlson, R. W., M. S. Anderson, R. E. Johnson, W. D. Smythe, A. R. Hendrix, C. A. Barth, L. A. Soderblom, G. B. Hansen, T. B. McCord, J. B. Dalton, R. N. Clark, J. H. Shirley, A. C. Ocampo, and D. L. Matson 1999a. Hydrogen peroxide on the surface of Europa. *Science* **283**, 2062-2064.
- Carlson, R. W., R. E. Johnson, and M. S. Anderson 1999b. Sulfuric acid on Europa and the radiolytic sulfur cycle. *Science* **286**, 97-99.
- Carlson, R. W., R. E. Johnson, M. S. Anderson, J. H. Shirley, M. Wong, S. Doute, and B. Schmitt 2001. Radiolytic influence on the surface composition of the galilean satellites (abstract). Jupiter: Planet, Satellites, and Magnetosphere, June 25-30, Boulder, CO, <http://lasp.colorado.edu/jupiter/index.html>.
- Clark, R. N., and P. G. Lucey 1984. Spectral properties of ice-particulate mixtures and implications for remote sensing 1. Intimate mixtures. *J. Geophys. Res.* **89**, 6341-6348.

- Cooper, J. F., R. E. Johnson, B. H. Mauk, H. B. Garrett, and N. Gehrels 2001. Energetic Ion and electron irradiation of the icy galilean satellites. *Icarus* **149**, 133-159.
- DellaGuardia, R. A., and F. J. Johnston 1980. Radiation-induced reaction of sulfur and water. *Radiation Res.* **84**, 259-264.
- Donaldson, G. W., and F. J. Johnston 1968. The radiolysis of colloidal sulfur. *J. Phys. Chem.* **72**, 3552-3558.
- Ershov, B. G., and A. K. Pikaev 1969. Stabilized free radicals in the radiation chemistry of frozen aqueous systems. *Radiation Res. Rev.* **2**, 1-101.
- Fender, M. A., Y. M. Sayed, and F. T. Prochaska 1991. Infrared-Spectrum of Sulfinic Acid HSO₂H in Solid Argon. *J. Phys. Chem.* **95**, 2811-2814.
- Geissler, P. E., R. Greenberg, G. Hoppa, A. McEwen, R. Tufts, C. Phillips, B. Clark, M. Ockert-Bell, P. Helfenstein, J. Burns, J. Veverka, R. Sullivan, R. Greeley, R. T. Pappalardo, J. W. Head, M. J. S. Belton, and T. Denk 1998. Evolution of lineaments on Europa: Clues from Galileo multispectral imaging observations. *Icarus* **135**, 107-126.
- Ghormley, J. A., and A. C. Stewart 1956. Effects of γ -radiation on ice. *J. Amer. Chem. Soc.* **78**, 2934-2939.
- Grundy, W. M., and J. A. Stansberry 2000. Solar gardening and the seasonal evolution of nitrogen ice on Triton and Pluto. *Icarus* **148**, 340-346.

- Hall, D. T., P. D. Feldman, M. A. McGrath, and D. F. Strobel 1998. The far-ultraviolet oxygen airglow of Europa and Ganymede. *Astrophys. J.* **499**, 475-481.
- Hall, D. T., D. F. Strobel, P. D. Feldman, M. A. McGrath, and H. A. Weaver 1995. Detection of an oxygen atmosphere on Jupiter's moon Europa. *Nature* **373**, 677-679.
- Head, J. W., R. T. Pappalardo, and R. Sullivan 1999. Europa: Morphological characteristics of ridges and triple bands from Galileo data (E4 and E6) and assessment of a linear diapirism model. *J. Geophys. Res.* **104**, 24223-24236.
- Hochanadel, C. J. 1960. Radiation chemistry of water. In: *Comparative Effects of Radiation*. (M. Burton, J. S. Kirby-Smith, and J. L. Magee, Ed.), pp. 151-189. Wiley & Sons, New York.
- Johnson, R. E. 2000. Surface chemistry in the jovian magnetosphere radiation environment. In: *Chemical Dynamics in Extreme Environments. Advanced. Series Phys. Chem.* (R. A. Dressler, Ed.), pp. 390-419. World Scientific, Singapore.
- Johnson, R. E., and W. A. Jesser 1997. O₂/O₃ microatmospheres in the surface of Ganymede. *Astrophys. J.* **480**, L79-L82.
- Johnson, R. E., M. L. Nelson, T. B. McCord, and J. C. Gradie 1988. Analysis of Voyager images of Europa - Plasma bombardment. *Icarus* **75**, 423-436.
- Johnson, R. E., and T. I. Quickenden 1997. Photolysis and radiolysis of water ice on outer solar system bodies. *J. Geophys. Res.* **102**, 10985-10996.

- Johnson, R. E., D. Schnellenberger, and M. C. Wong 2000. The sputtering of an oxygen thermosphere by energetic O^+ . *J. Geophys. Res.* **105**, 1659-1670.
- Kargel, J. S., J. W. Head III, D. L. Hogenboom, K. K. Khurana, and G. Marion 2001. The system sulfuric acid - magnesium sulfate - water: Europa's ocean properties related to thermal state (abstract), Lunar and Planetary Science Conference XXXII. Lunar and Planetary Institute, Houston, CD-ROM Abstract No. 2138.
- Kargel, J. S., J. Kaye, J. W. I. Head, G. Marion, R. Sassen, J. Crowley, O. Prieto, and D. Hogenboom 2000. Europa's crust and ocean: Origin, composition, and prospects for life. *Icarus* **94**, 368-390.
- Lane, A. L., R. M. Nelson, and D. L. Matson 1981. Evidence for sulfur implantation in Europa's UV absorption band. *Nature* **292**, 38-39.
- Makarov, S. V., C. Mundoma, J. H. Penn, S. A. Svarovsky, and R. H. Simoyi 1998. New and surprising experimental results from the oxidation of sulfinic and sulfonic acids. *J. Phys. Chem. A* **102**, 6786-6792.
- Marion, G. 2001. A molal-based model for strong acid chemistry at low temperatures (187 to 298 K). *Geochimica et Cosmochimica Acta* to be submitted.
- Martin, L. R., and D. E. Damschen 1981. Aqueous oxidation of sulfur dioxide by hydrogen peroxide at low pH. *Atmos. Environ.* **15**, 1615-1621.

- McCord, T. B., G. B. Hansen, D. L. Matson, T. V. Johnson, J. K. Crowley, F. P. Fanale, R. W. Carlson, W. D. Smythe, P. D. Martin, C. A. Hibbitts, J. C. Granahan, A. Ocampo, and a. t. N. Team 1999. Hydrated salt minerals on Europa's surface from the Galileo NIMS investigation. *J. Geophys. Res.* **104**, 11827-11851.
- Meyer, B., T. V. Oommen, and D. Jensen 1971. The color of liquid sulfur. *J. Phys. Chem.* **75**, 912-917.
- Moore, M. H. 1984. Studies of proton-irradiated SO₂ at low-temperatures - Implications for Io. *Icarus* **59**, 114-128.
- Moore, M. H., and R. L. Hudson 2000. IR detection of H₂O₂ at 80 K in ion-irradiated laboratory ices relevant to Europa. *Icarus* **145**, 282-288.
- Moorthy, P. N., and J. J. Weiss 1964. Radiation-induced formation of the univalent Mg⁺, Zn⁺, and Cd⁺ from the divalent cations in γ -irradiated ice. *Nature* **201**, 1317-1318.
- Nash, D. B., and F. P. Fanale 1977. Io's surface composition based on reflectance spectra of sulfur/salt mixtures and proton irradiation experiments. *Icarus* **31**, 40-80.
- Noll, K. S., H. A. Weaver, and A. M. Gonnella 1995. The albedo spectrum of Europa from 2200 angstrom to 3300 angstrom. *J. Geophys. Res.* **100**, 19057-19059.
- O'Donnell, J. H., and D. F. Sangster 1970. *Principles of Radiation Chemistry*. American Elsevier, New York.

Paranicas, C., R. W. Carlson, and R. E. Johnson 2001. Electron bombardment of Europa.

Geophys. Res. Lett. **28**, 673-676.

Rothschild, W. G. 1964. γ -Ray decomposition of pure liquid sulfur dioxide. *J. Am. Chem. Soc.*

86, 1307-1309.

Sasaki, T., R. S. Williams, J. S. Wong, and D. A. Shirley 1978. Radiation damage studies by x-ray photoelectron spectroscopy. I. Electron irradiated LiNO_3 and Li_2SO_4 . *J. Chem. Phys.*

68, 2718-2724.

Schumb, W. C., C. N. Satterfield, and R. L. Wentworth 1955. *Hydrogen Peroxide. American Chemical Society Monograph Series* Reinhold, New York.

Shirley, J. H., R. W. Carlson, and M. S. Anderson 1999. Upper limits for magnesium and sodium hydroxides on Europa (abstract). *EOS, Trans., Amer. Geophys. Union* **80**, No. 46, F604.

Spencer, J. R., and A. Klesman 2001. New observations of molecular oxygen on Europa and Ganymede (abstract). *Bull. Amer. Astron. Soc.* **33**, 1125.

Spencer, J. R., L. K. Tampari, T. Z. Martin, and L. D. Travis 1999. Temperatures on Europa from Galileo photopolarimeter-radiometer: Nighttime thermal anomalies. *Science* **284**, 1514-1516.

Taub, I. A., and K. Eiben 1968. Transient solvated electron, hydroxyl, and hydroperoxy radicals in pulse-irradiated crystalline ice. *J. Chem. Phys.* **49**, 2499-2513.

- Vairavamurthy, M. A., and W. Q. Zhou 1995. Characterization of a transient +2 sulfur oxidation state intermediate from the oxidation of aqueous sulfide. In: *Geochemical Transformations of Sedimentary Sulfur. ACS Symposium Ser.*, pp. 280-292. Amer. Chem. Soc., Washington D. C.
- Wourzel, E. 1920. Actions chimiques du rayonnement α . *J. Phys. Radium* **1**, 77-96.
- Yung, Y. L., and W. B. DeMore 1982. Photochemistry of the stratosphere of Venus: Implications for atmospheric evolution. *Icarus* **51**, 199-247.

TABLE

Table I. Radiolysis rates and lifetimes. G -values and rates of decomposition, $G(-X)$ and $v(-X)$, and the corresponding lifetime, $\tau(-X)$, are shown in bold. Individual reactions and rates are also shown.

Species, X and reaction pathways (reference and notes)	G_1 (100 eV) ⁻¹	Rate v 10 ⁻⁹ s ⁻¹	Lifetime, τ years
Sulfur, S	0.4(r_0/r)^{1.9}	0.3(r_0/r)^{1.9}	120(r/r_0)^{1.9}
S ₈ + H ₂ O \rightsquigarrow H ₂ SO ₄ (a)	0.4(r_0/r) ^{1.9}	0.3(r_0/r) ^{1.9}	
Sulfur Dioxide, SO₂	5	7	5
SO ₂ \rightsquigarrow SO ₃ (b) \rightarrow H ₂ SO ₄ (c)	4.5	6	
SO ₂ \rightsquigarrow S (c, d)	0.7	0.9	
Hydrogen Sulfide, H₂S	8	6	6
H ₂ S \rightsquigarrow S (e)	8	6	
Sulfates, SO₄²⁻ (f)	0.004	0.008	3800
H ₂ SO ₄ \rightsquigarrow SO ₃ ²⁻ (g) \rightarrow HSO ₄ ⁻ \rightarrow SO ₂ (h)	0.0034	0.0070	
H ₂ SO ₄ \rightsquigarrow S ²⁻ (g)	0.00064	0.0013	
H ₂ SO ₄ \rightsquigarrow S (g)	0.00008	0.0002	

(a) Present results. (b) Proton irradiation, (Moore 1984). (c) SO₃ + H₂O rapidly produces H₂SO₄, (Carlson *et al.* 1999b). (d) Liquid-state value, (Rothschild 1964). (e) (Wourtzell 1920). (f) These values are representative of both acid and salt sulfates. The lifetime is an upper limit because cation removal is not included. (g) (Sasaki *et al.* 1978). (h) Sulfite decomposes to SO₂ under acidic conditions.

FIGURE CAPTIONS

Fig. 1. Europa's radiolytic sulfur cycle. Stable species are represented by the rectangles and the transient intermediary, sulfinic acid, by the circle. Radiolysis paths are indicated by the arrows and the corresponding reaction rate (G -value) is indicated for unit concentration. The $S + H_2O \rightsquigarrow SO_2H_2 \rightsquigarrow H_2SO_4$ rate, measured in this work, is grain-size dependent; the value shown is for 50- μm radius S_8 grains exposed to energetic electrons. Decomposition lifetimes range from 5 years (SO_2) to 3800 years (SO_4^{2-}) so the overall cycle time is ~ 4000 years. See Table I for rates and lifetimes.

Fig 2. Ion chromatograms for 77 K irradiated (top) and unirradiated (bottom) heterogeneous S_8 frozen aqueous mixtures. In each case, samples with 0, 5, 10, and 15 wt-% sulfur were identically treated. The sulfate increase due to irradiation is evident, and a nitrate impurity is found for both the irradiated and unirradiated samples. No sulfite was observed.

Fig. 3. Sulfate produced by irradiation. The SO_4^{2-} weight fraction generated by radiolysis is approximately linearly dependent on the initial weight fraction of sulfur. The lines represent linear least-squares fits and $\pm 1-\sigma$ deviations from the fits. Irradiation at 77 K produces more sulfate than does irradiation at 195 K. The doses for these irradiations were ~ 100 krad.

Fig. 4. Sulfate production dose dependence. Heterogeneous solutions ($f_{\text{Sulfur}} = 15\%$) at 77 K were exposed to a ^{60}Co source for periods up to 72 hours. Sulfate concentrations of the exposed samples, minus the concentrations of the unexposed samples, are shown (filled circles) and compared to the unexposed values (open circles). The sulfate production is consistent with the linear dose dependence indicated by the fitted line. The sulfate production rate in this experiment is $\sim 40\%$ of the $r_0 = 50 \mu\text{m}$ value (Fig. 3). This may be due to the $r^{-1.9}$ G -value variation and the larger effective size of the particles, which were found to be aggregates with $r = 50$ to $250 \mu\text{m}$.

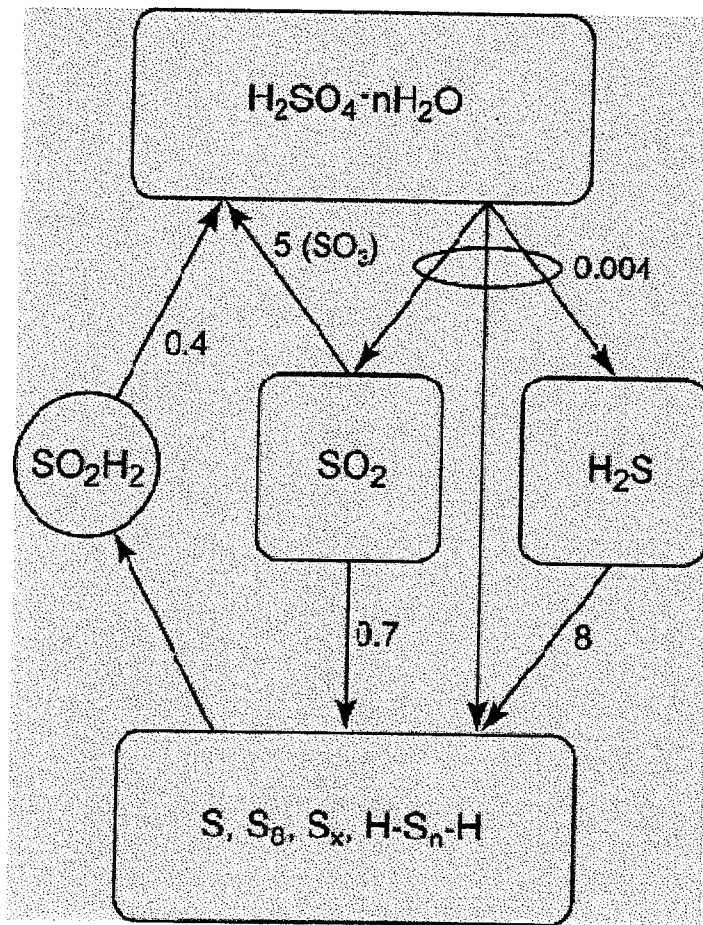


Fig. 1.

Carlson et al.

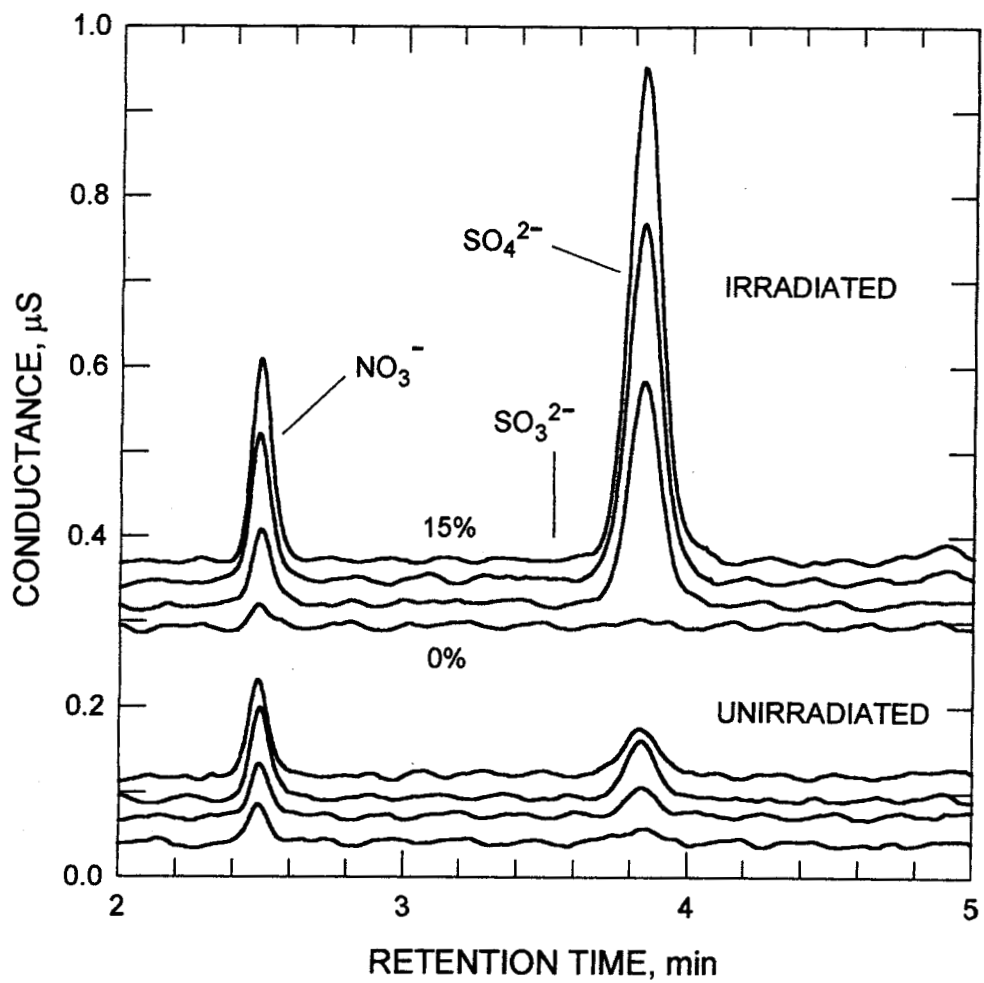


Fig. 2

Carlson et al.

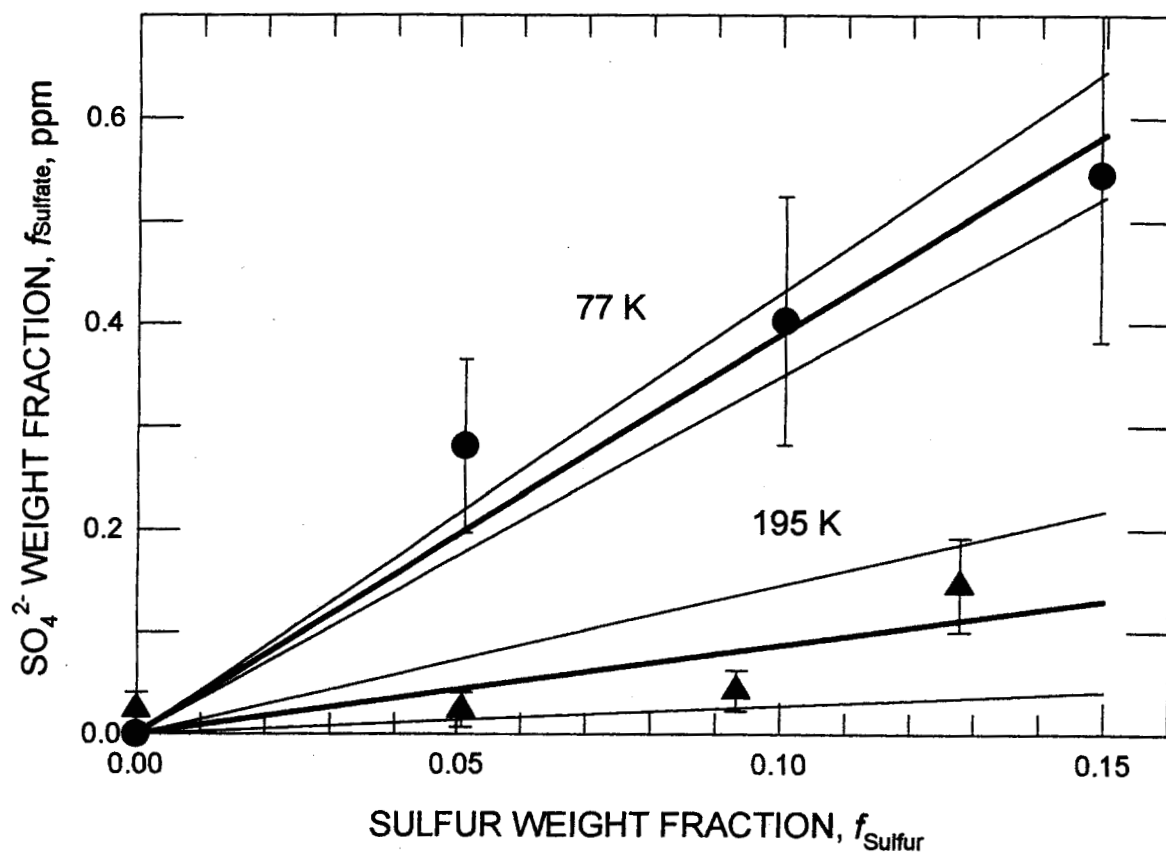


Fig. 3.

Carlson et al.

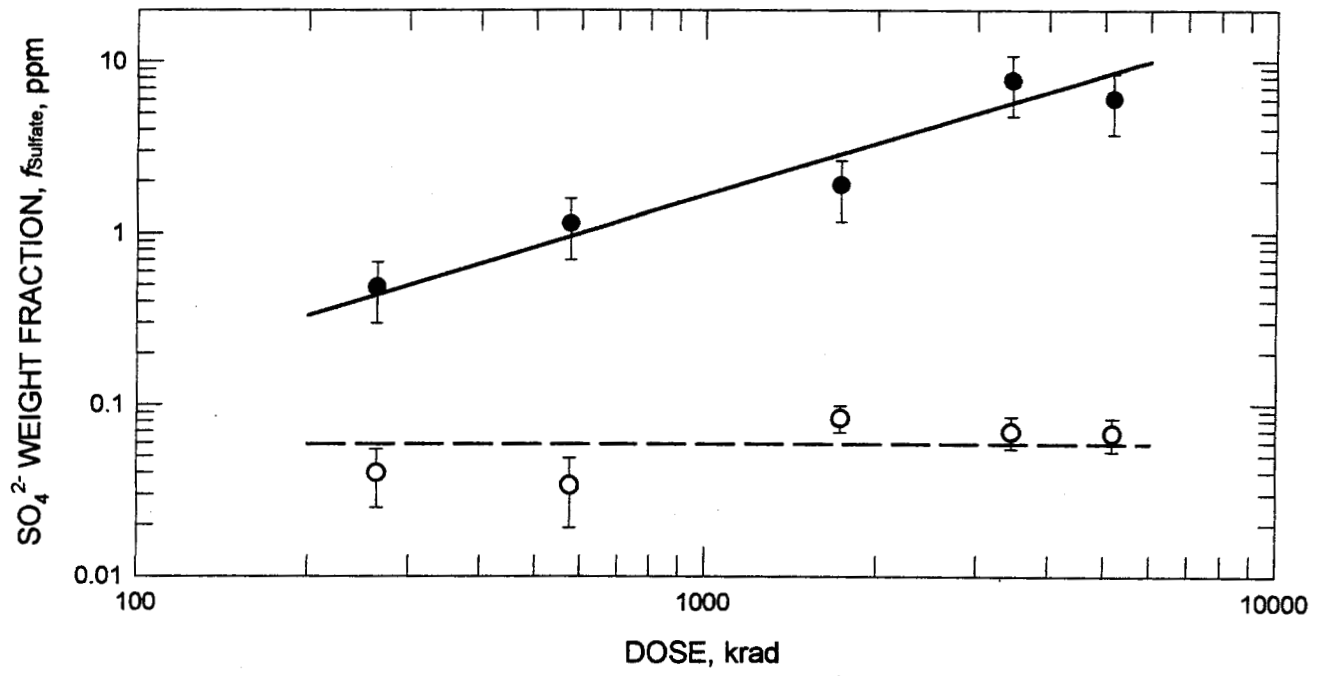


Fig. 4.

Carlson et al.